Open Access
Original paper

Budownictwo i Architektura / Civil and Architectural Engineering 25(2) (2026) 26025
https://doi.org/10.35784/bud-arch.8638

Stress-strain response of quaternary sand mixed with granulated rubber under restraint condition

Abbas J. Al-Taie[1,*], Mahmood Ahmed[2]

[1] *Department of Civil Engineering; College of Engineering; Al-Nahrain University; Al-Jadriya, 10070, Baghdad, Iraq; and Department of Civil Engineering; College of Engineering; University of Baghdad; Al-Jadriya, 10070, Baghdad, Iraq; abbas.j.al-taie@nahrainuniv.edu.iq; al.taiegeo@gmail.com*
[2] *Department of Civil Engineering; College of Engineering; University of Baghdad; Al-Jadriya, 10070, Baghdad, Iraq; dr.mahmood.da@coeng.uobaghdad.edu.iq*

[*] *Corresponding Author*
Received: 27.10.2025; Revised: 11.03.2026; Accepted: 13.03.2026; Available online: 26.06.2026

Abstract:
The Quaternary soils, QS, are considered widespread materials found near or at the Earth's surface. Despite their engineering characteristics, they are characterised by low vibration damping. On the other hand, materials such as rubber tyre waste (TW) exhibit greater damping capacity. Such material is problematic in the surrounding environment and causes critical hazards. Mixing these materials yields composite geomaterials with distinct characteristics for varied geotechnical applications and helps address many challenges associated with them. To ensure the benefits outweigh the likely risks, systematic testing of the Quaternary Soil-Rubber Tyre Waste (QSTW) mixtures is crucial. The current study surveys the responses of QSTW mixtures under confined-restraint conditions. For laboratory specimens' preparation, different weight fractions of the TW were mixed, in the dry condition, with the QS (0.0, 15.0, 30.0, 45.0, and 100.0%). The volume deformability, stiffness, and energy dissipation were produced from testing these specimens under zero lateral strain in dry and saturated states. The results indicate that the mixtures of QSTW suffer more deformation and become less stiff with increasing rubber inclusion. Such inclusion permits the grains' rearrangement and allows additional replacement from the solid skeleton, producing different packing. The degree of the nonlinearity of the stress-strain curves increases with higher TW, and the mixtures' response seems "rubber – like" at higher content. In contrast, the absorption and the energy dissipation of the QS augment with the TW inclusion, where the TW acts as a mini damper within the mixtures. These mixtures show high capacity for vibration-damping and thus can be applicable for various infrastructures subjected to vibrations.

Keywords:
quaternary soils; tyre waste; energy dissipation; stiffness; confined compression

1. Introduction

The geologists assume the Quaternary soil, QS, is the most prevalent material found on the Earth's surface, or close to it. This soil has special characteristics that make it suitable as material for various engineering infrastructures [1,2]. These characteristics are related to parent material types, depositional processes, and resulting engineering behaviour, which influence their engineering behaviour. It has been demonstrated that the QS can be used as backfill for retaining structures and as fill material beneath their footings [3,4]. Developing systematic engineering methods to exploit these abundant deposits can expand their engineering applications.

Furthermore, rubber tyre waste, or TW, from scrap tyres accumulates daily and poses significant risks and problems to the environment. To identify workable ways to address these materials' issues, numerous studies have been carried out [5,6]. They employed a variety of recycled tyre forms (including granulated solids, chips, and shreds) in various civil infrastructure applications (e.g., improving the material incorporated into asphalt mixtures [7,8], concrete beams [9], lightweight geomaterials [10], foundation layers [11]).

When these materials are combined with soils, unique geomaterial mixtures are created. These materials are useful in a number of civil engineering projects. These uses include thermal insulation in roadways [12], drainage applications [13,14], vibration damping for foundations [15,16], minimising building heat losses [17], and using lightweight geomaterials as backfill for earth-retaining walls and fill for highway embankments [10], [18–21].

Engineered combinations of granular materials may exhibit unique properties. Mixtures of sand and rubber materials have been studied by several researchers. The increasing volume of waste tyres necessitates such investigations [22–24]. These investigations can help uncover additional specific applications and provide specifications to facilitate construction and environmental protection [25]. Mixtures of granular materials and rubber have been proposed by scholars for isolation applications to reduce the seismic impact on foundations [26–28]. Pitilakis et al. [29], Maleska et al. [30] proposed the mixtures of gravel and rubber as one of these materials. They described them as high-damping materials with reduced shear stiffness and, therefore, as eco-sustainable materials for infrastructure.

According to Bernal et al. [31], confined compression tests on sand reinforced with shredded tyre material (3.81 cm in size) and compacted in a 15.2 cm mould indicated that compressibility increases significantly when the tyre shred content exceeds 30 % (by weight of sand). The primary compression components of these mixtures are irrecoverable, with some rebound denoted during the load release [32]. The water absorption of shredded tyre material, as stated by Humphrey and Manion [33] and Humphrey et al. [34], is very limited. It has an average unit weight of 6.17 kN/m^3, a strength angle of 19 to 25 degrees, and

a cohesion intercept of (between 7.7 and 11.5 kPa). These authors investigated the compressibility of shredded tyres during loading and unloading cycles. They stated that compressibility decreases with increasing number of loading-unloading cycles.

The interaction between sand and rubber particles and the mechanisms of energy dissipation were investigated by Fonseca et al. [35]. They utilised X-ray tomography and oedometer tests to explain energy dissipation and support the idea that the contribution of rubber becomes more significant at higher applied stresses. Moreover, these authors showed the influence of saturation on frictional sliding. These authors claim that oedometer loading – unloading curves can be used to assess energy dissipation at high strain levels. On the other hand, Wu et al. [36] used resonant column tests to examine the dynamic behaviour of sand-rubber mixtures at low strain. The idea of "increasing the rubber content enhances the damping capacity" was validated by their analysis. While the damping ratio and the shear modulus of the granular soil mixed with up to 35% rubber were studied by Anastasiadis et al. [37] using the "torsional resonant column tests." They found that, at small strain, the size and proportion of rubber used have a significant impact on the dynamic properties.

The impact of cyclic axial loading on sand–rubber mixtures is examined by Ozkan et al. [38]. Their experimental program employed one-dimensional loading tests to report the damping behaviour, hysteresis loops, and stiffness degradation under cyclic axial loading. This investigation showed that energy dissipation varies with loading cycles, rubber content, and applied stress. In contrast, Tao et al. [39] investigate the damping of sand-rubber mixtures by exposing them to cyclic loading. Their analysis demonstrated that damping during dynamic vibrations reflects the material's energy-dissipation capacity.

Additionally, Li et al. [40] investigated the energy dissipation behaviour of sand combined with rubber material. The damping behaviour and energy dissipation of mixtures under cyclic triaxial loading were investigated by these authors. They discovered that the amount of rubber had a substantial effect on the energy dissipated; they also concluded that increasing the proportion of rubber leads to higher energy dissipation. Polito et al. [41] and Polito and Martin [42] examined the energy dissipation behaviour of clean sand with silt subjected to cyclic loading using various tests, including cyclic simple and cyclic triaxial tests (both stress- and strain-controlled). They discovered that the proportion of energy dissipated depends on the magnitude of the applied energy and is not influenced by the duration of dissipation. Fiamingo et al. [6] used triaxial tests to highlight the potential applications of the mixtures of granular soils and shredded rubber. They examined the energy absorption and the paths of stress and strain in these materials toward failure under drained conditions. The important contribution from their study, in the context of the reviewed literature, is the substantial effect of the amount of rubber on both the amount and pattern of energy dissipation. The amount of energy dissipated in turn can reflect damping during dynamic vibrations. Furthermore, the damping behaviour, hysteresis loops, and stiffness degradation can be reported from the adopted one-dimensional loading tests.

There is a high similarity between the "volumetric stress – strain" relationships of geomaterials during both confined compression and isotropic conditions. In practice, confined compression is the more common condition in nature. Soil formation by sedimentation is an example of this condition. Similarly, soils are under confined compression when they are subjected to vertical stresses with a large lateral extent. In nature, as stated by Lambe and Whitman [43], it is seldom that one encounters isotropic compression. Furthermore, the performance of an experimental test to represent the confined compression condition is easier and can be efficiently performed using oedometer tests. The preceding review highlights that there are relatively few systematic experimental studies on the stiffness, collapse, and energy dissipation of sand-rubber specimens utilising the oedometer apparatus in the literature.

To address this gap, the present experimental investigation was designed to explore in more detail the compressibility, stiffness, collapsibility, and energy dissipation of "Quaternary soil, QS" and its mixtures with rubber, from tyre waste (TW), under lateral restraint conditions. Three series of oedometer tests were conducted for pure QS specimens, QS mixed with (15, 30, and 45%) tyre waste (TW), and specimens of pure TW. The tests include, in addition to standard physical tests, standard oedometer tests, double oedometer tests, and cyclic oedometer tests performed under both dry and saturated conditions.

2. Materials and methods

Quaternary soil (QS) from the centurial Mesopotamian Plain is used in this study. The selected material is a fine, uniform, brownish-grey sand. The main physical properties of this soil, listed in Table 1, show that it is fine-sized, poorly graded sand as per USCS, the "Unified Soil Classification System," ASTM D2487 [49]. The SEM images (Fig. 1) show that the QS grains have low sphericity, are bulky, and range from subangular to slightly rounded. The kind of parental grain materials and the length of the route they transported are among the main factors that affect the rounding degree of these grains. Accordingly, as the QS grains are transported over long distances via the action of the Rivers "Tigris and Euphrates," they are "sub-angular" to "slightly rounded". This characteristic may influence the soil's engineering behaviour.

Also, the rubber tyre waste, TW, in the form of granulated rubber tyre from the recycling of scrap tyre waste, was utilised. This waste material is a black-coloured, poorly graded, sand-sized particle with a low solid density, as illustrated in Table 1.

The preparation of the quaternary soil and the rubber tyre waste mixtures involves various weight fractions (W_f) of TW (ranging from 0 to 100%). W_f was calculated using the expression in Eq. 1 (W_{TW} and W_{QS} are the dry weight of the rubber tyre waste and quaternary soil, respectively). In the first mixture, the W_f is 0%, indicating a pure quaternary soil (without rubber) and is denoted as (QSTW0). In the latest mixture, W_f is 100%, indicating the material is pure rubber tyre waste (designated as QSTW100). The remains of the W_f values are (15%, 30%, and 45%), and are designated as (QSTW15, QSTW30, and QSTW45), respectively.

$$W_f = \frac{W_{TW}}{W_{TW} + W_{QS}} \times 100 \quad (1)$$

The limiting unit weights of the mixtures of quaternary soil and rubber tyre waste were determined following the procedures outlined in ASTM standards [48,49]. The limiting values were used to obtain the limiting void ratios. The relative density, Dr, adopted for the oedometer tests' specimens was 75 %. As a result, the void ratio required for each mixture was specified.

Table 1. The properties of the experimental materials

Properties		Standards [44–50]	Quaternary soil	Tyre Waste
Colour		-	brownish grey	black
Specific gravity, Gs		ASTM D854	2.68	1.32
Particles size distribution	Gravel size, %	ASTM D422	0	0
	Sand size, %	ASTM D422	97	100
	Fine materials, %	ASTM D422	3	0
Unified soil classification system (USCS), or identification	D50, mm	ASTM D2487	0.2	2.0
	Cu	ASTM D2487	0.97	3.35
	Cc	ASTM D2487	1.77	1.25
	USCS/Identification	ASTM D2487/D2488	SP	Sand-sized
Limiting unit weights	γ_{min} /γ_{max}	ASTN D4253	0.94	0.89
		ASTMD4254		

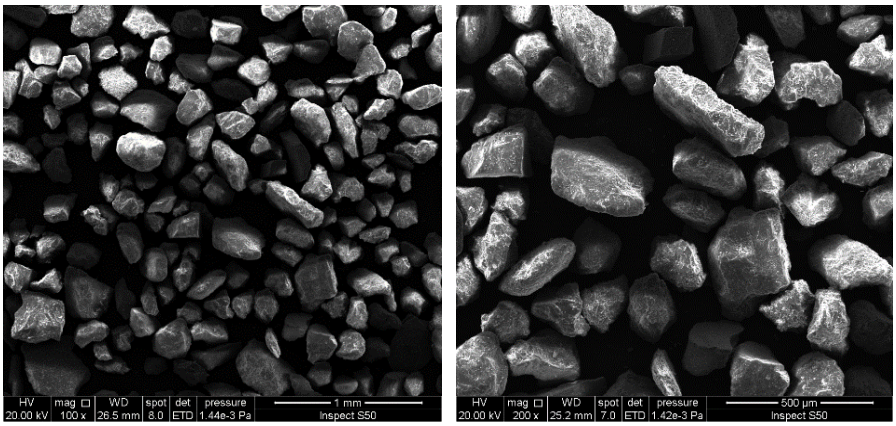

(a) (b)

Fig. 1. SEM images a; scale of 100; b; scale of 200

In this experimental work, different types of oedometer tests were conducted employing the standard apparatus with front-loading. The prepared specimens are 50 mm in diameter and 20 mm in height. The mixtures were first divided into two parts, then placed in a clean, lubricated stainless steel ring and fixed in the oedometer cell. This is to mitigate the influence of boundary friction and segregation. A tamper rod of steel of 5 mm in diameter, a steel-made bowl and spoon, and a digital scale of sensitivity 0.01 g were used to obtain the target Dr For each mixture, the Dr. was specified, the corresponding unit weight calculated, and then the weight of material required to fit the full volume of the oedometer cell's ring was determined. The required material weight was prepared as a dry mixture inside the steel bowl fairly and carefully until it looked as homogeneous as possible, as presented in Fig. 2. Afterwards, from a falling distance of zero, the homogenous dry mixture was translated into the inside of the oedometer ring in two steps; an equal part of the mixture was used in each step. Herein, any possible segregation was averted. The specimens were tamped with the steel tamper until the dry mixture reached the oedometer ring volume. The oedometer was set up, an initial setting load of 5 kPa was applied, and the dial gauge (with a sensitivity of 0.002 mm) was adjusted to an initial reading. The laboratory station for the current work is the central laboratory of the Civil Engineering Department of the University of Baghdad (Fig. 3).

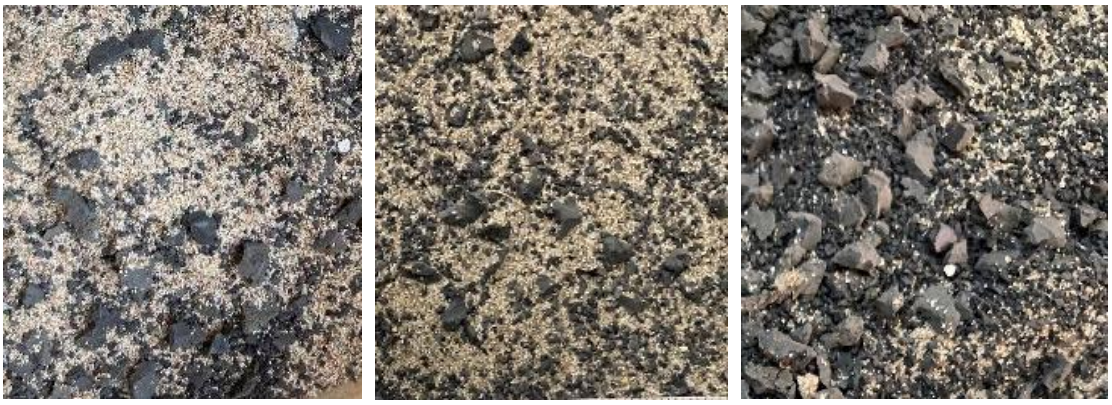

(a) QSTW15 (b) QSTW30 (c) QSTW45

Fig. 2. Quaternary soil-rubber tyre waste mixtures

Fig. 3. Pictures of the apparatus used in the research station of the current work

In this study, three oedometer test series were conducted for each mixture. The prepared specimens in the first series were compressed in both the dry state and after saturation with tap water (inundation for 24 hrs.). The saturated water content was measured after the immersion period. The measured water content values were used to determine the degree of saturation for each specimen and ensure the required saturation condition was met. The specimens in both states were subjected to applied stresses in accordance with ASTM D2435 [49]. The primary objectives of this series were to evaluate the compression parameters, compressibility behaviour, and stiffness of the mixtures.

The second series was focused on the potential collapse under a double oedometer loading. Identically prepared specimens were loaded as per Jennings and Knight's [51] procedure, one in a dry state and the other in an inundation with tap water.

In the final series, a non-classical confined compression test was conducted. To investigate the energy dissipation and stiffness of the dry and saturated Quaternary soil and rubber tyre waste mixtures under different cycles of loading – unloading – reloading, cyclic oedometer tests were carried out. This series aims to provide comments on the dynamic responses of these materials. It should be noted that the procedure adopted in this test series is as per Fonseca et al. [35]; Ozkan et al. [38]; Edil and Bosscher [52]; and Ozkan et al. [53]. The initial specimens were prepared under standard oedometer conditions and an initial setting load of 5 kPa, but with loading in a different particular order. Firstly, the specimens were loaded to a specified stress, then unloaded (in an unloading stage) to the initial loading stress. Then, the specimens were reloaded in a reloading stage with an applied load ordering similar to the last stage, but with an applied stress twice the previous stress. The stated stages (i.e., loading, unloading, and reloading) represent one loop of applied stress. These stages were repeated by increasing the stress increment to create more loops. A schematic diagram of the loading – unloading stress path is presented in Fig. 4. It is worth noting that each specimen underwent five cycles and was tested in both the dry and saturated states to reconnoitre the cyclic response under inundation conditions.

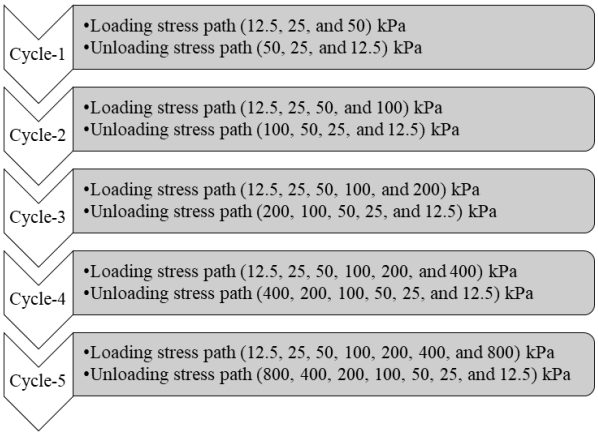

Fig. 4. Schematic diagram for loading–unloading stresses in cyclic oedometer test

3. Results and discussions

The limiting densities (maximum and minimum) and the corresponding void ratios of QS – TW mixtures were calculated and presented in Fig. 5. The highest maximum and minimum void ratios were observed for pure rubber tyre waste, 1.309 and 1.052. This provides a good indication of TW's damping characteristics. Incorporating TW into QS reduced the solid densities of the resulting mixtures and altered the void ratios. This is due to replacing the solid grains of the QS with the soft TW grains. This may affect the mixtures' responses to compressibility and damping characteristics, as discussed later. In the context of this effect, the results of oedometer tests on Quaternary soil-rubber tyre waste mixtures under lateral resistant conditions are analysed and plotted, taking into account the impact of TW contents on the compressibility, stiffness, collapse potential, and energy dissipation of QSTW mixtures at different states.

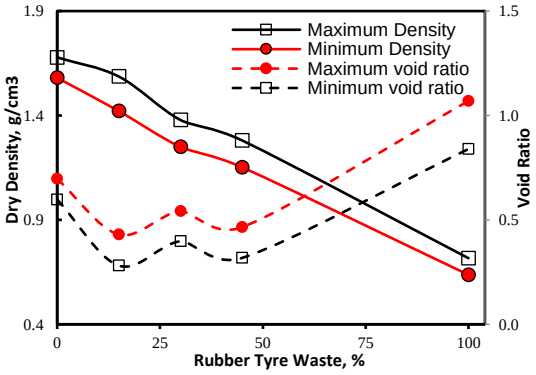

Fig. 5. Effect of rubber tyre waste on the limiting of Quaternary soil

3.1. Rubber tyre waste effects on the compressibility

Under the "one-dimensional confinement" condition, the compressibility of dry and soaked mixtures of Quaternary soil (QS) – rubber tyre waste (TW) was studied. The outcome of the oedometer test is presented in Fig. 6 for the diversity of TW content utilised in this work, in the form of axial strain (%, normal scale) vs. the effective normal stress (kPa, logarithmic scale). As shown, the vertical strain of pure QS samples remains limited, even at high stress levels. Furthermore, the near-linear response is clear in the stress-strain curves.

The compressibility curves exhibit strong nonlinearity at high TW fractions and high stress levels. On the other hand, at TW content above 15%, the response shows distinct rebound curves at higher applied stresses. This is also noted for sandy soil samples tested by other scholars [54–57]. The recorded amount of rubber, in the literature, in which a similar behaviour was noted, is greater than 20% [52,53,58–60].

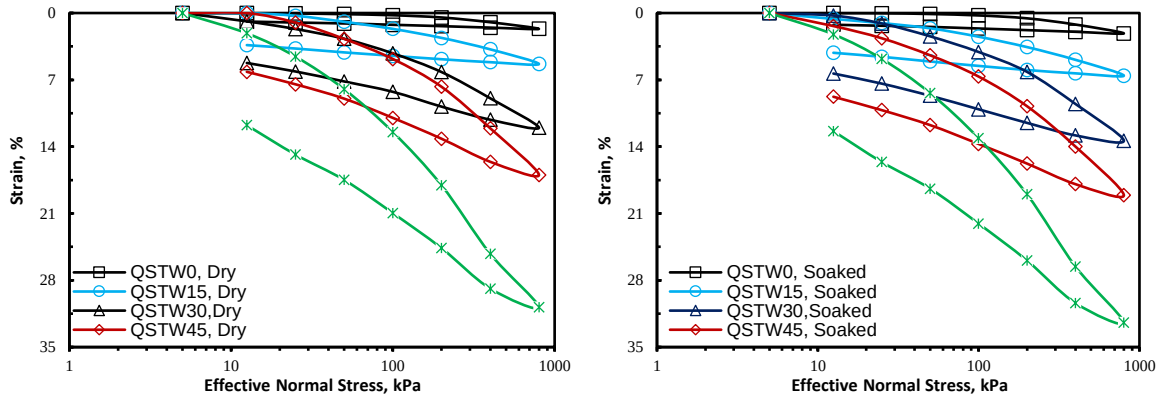

Fig. 6. Compressibility curves for QSTW mixtures at dry and saturated states

The Quaternary soil mixed with rubber tyre waste reveals little sensitivity to wetting. In contrast, greater deformability is observed at higher TW content, where the minimum void ratio approaches 0.2. Furthermore, at the end of the unloading stages, higher values of the remnant strain are observed. This increase with higher rubber content due to the compressible and elastic nature of the TW particles.

The effect of the rubber inclusion on the compression parameters is explored in the current work. Figure 7 shows the variation in compression index (Cc) and rebound index (Cr) with TW content for both dry and soaked conditions. The compressibility parameters are directly proportional to TW content. The relationship between these parameters is highly linear, with excellent coefficient of determination values (R2 > 98%). Finally, it can be stated that the axial strain of QS–TW mixtures under confined loading increases as the material composition transitions from rigid, pure sand grains to more elastic and deformable rubber particles.

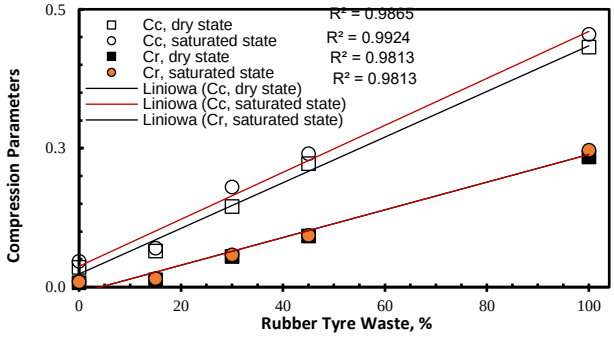

Fig. 7. Effect of rubber tyre waste on compression parameters

3.2. Rubber tyre waste effects on the mixture's stiffness

Investigating the stiffness of QSTW mixtures as a function of TW is a primary objective of the present study. Thus, the outcome of the oedometer test has been replotted in Fig. 8, showing effective normal stress (kPa) versus axial strain (%) on a linear scale for both axes. Unsurprisingly, the QSTW mixtures show a softer response than the pure QS. As the TW increased, the non-linearity of the curves was augmented due to the elastic deformability and less stiffness of TW grains. The slopes of the curves in Fig. 8 were used to calculate the "one-dimensional incremental confined stiffness (SM)" using Eq. 2 [43,53,61].

$$S_M = \frac{\Delta\sigma_v}{\Delta\varepsilon_v} \tag{2}$$

where "Δσ and Δε" are the stress increment and strain increment for each specimen. As per Muir-Wood [58], the form of Eq. 3 shown below can be applied to relate the following parameters: the S_M and effective normal stresses.

$$\frac{S_M}{\sigma_a} = b_1 \left(\frac{\sigma_v}{\sigma_a}\right)^{b_2} \tag{3}$$

where σ_a corresponds to 100 kPa and serves as a reference stress. The parameters b_1 and b_2 are the "modulus number" and parameter of "stiffness stress dependency," respectively [38,53]. The σ_a was utilised in the normalisation of S_M and σ_v. The stress and strain values for the current experiments were adopted to develop the form of the relation shown in Fig. 9. As shown, for

the dry and inundated conditions, the influence of TW is noticeable for inclusions at 30 % or above. where the curves are grouped together. This means that the value and the rate of augmentation in mixture stiffness are at their lowest state. Accordingly, the behaviour of the mixtures increasingly resembles that of pure rubber waste compared to pure granular soi. Ozkan et al. [53] and Madhusudhan et al. [62] indicated a similar trend for sandy soil mixed with high inclusions of shredded tyre or rubber material.

Muir-Wood [58] demonstrated that a decrease in the modulus number corresponds to lower material stiffness. The stiffness of QSTW mixtures is evaluated in this work using the values of the parameters b_1 and b_2 as illustrated in Fig. 10. Two distinct behaviours can be identified in Fig. 10: 'sand-like' and 'rubber-like [36,55,63]. For mixtures with a lower TR inclusion (≤15%), the recognised behaviour is the 'sand-like'. But with TR content greater than 30%, the mixtures exhibit behaviour closer to that of pure rubber. At higher TW content, rubber particle contacts dominate. This means dominance of rubber-like behaviour, with the magnitude of parameter b1 at a minimum, and vice versa. In contrast, the stiffness stress-dependency parameter increases proportionally with the rubber content. The value of this parameter is close to unity when the TW content exceeds 45%. This trend would indicate a proportional relationship between the constrained modulus and the level of stress. However, the stiffness of the mixture increases with decreasing TW inclusion, and soaking has a slight effect on the stiffness of QSTW mixtures.

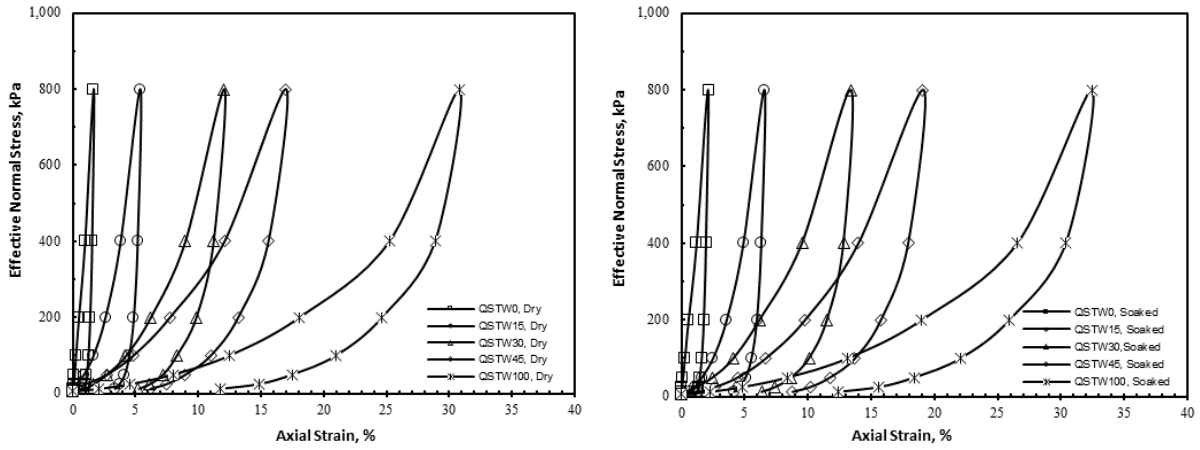

Fig. 8. Variation of axial strain vs. σv for different TW content

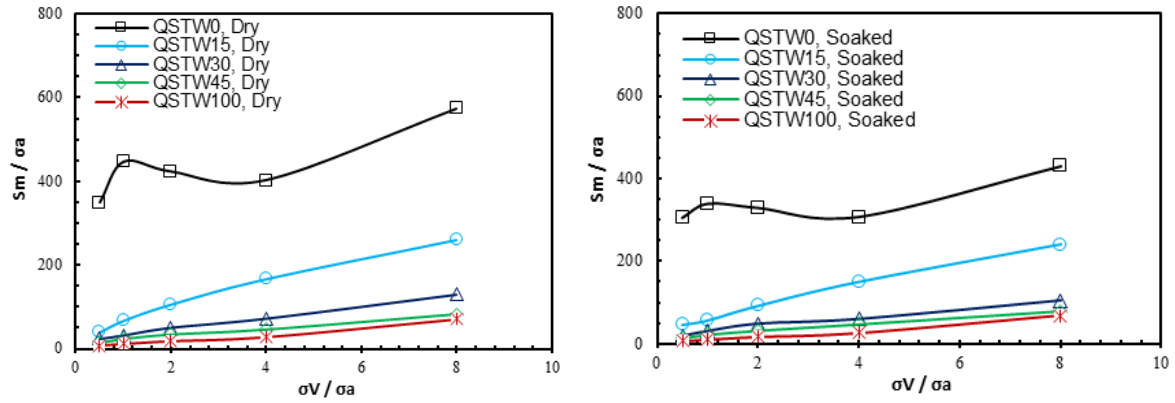

Fig. 9. Normalised SM vs. σv for various TW content

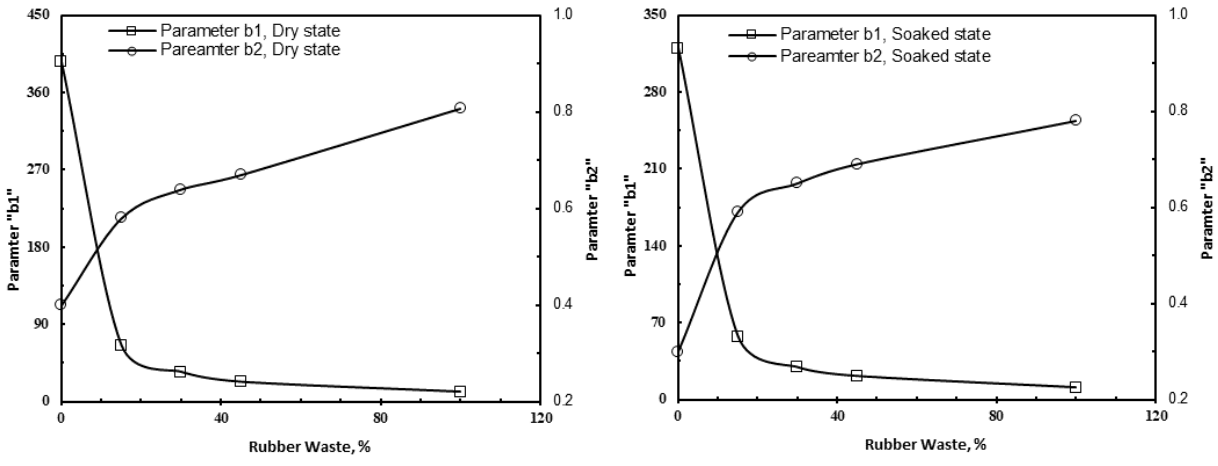

Fig. 10. Parameters b_1 and b_2 versus TW content for dry and soaked states

According to Muir-Wood [58], the geomaterials can be distributed in the form shown in Fig. 11. They are distributed based on their stiffness parameters (stiffness exponent and modulus number). In the present study, the effect of rubber waste inclusion on the position of QS – TW mixtures within these charts is evaluated. The parameters b_1 and b_2 are superimposed on this chart, the symbols in red. As shown, the inclusion of more TW causes an upward shift in b_2 and a downward shift in b_1. In other words, the mentioned movement indicates a change in the mixture's behaviour from stiffer and sand-like to softer and rubber-like. Nevertheless, all mixtures remain within the limits of defined geomaterials.

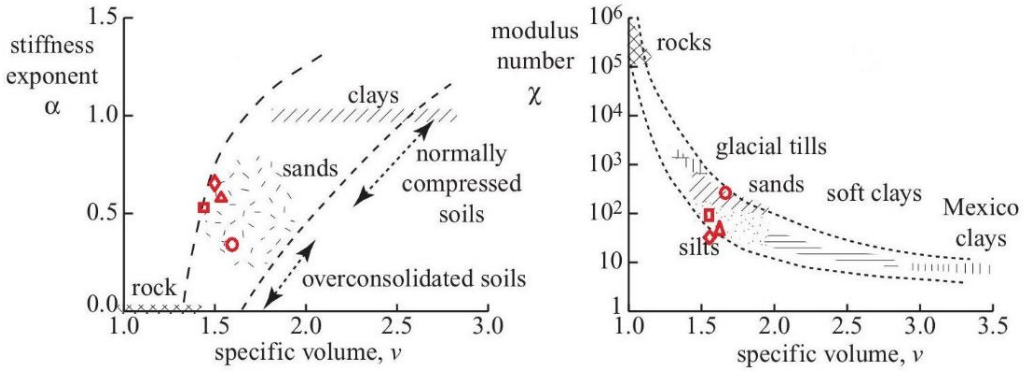

Fig. 11. Stiffness parameters for QSTW mixtures over those of different geomaterials Source: [58]

3.3. Rubber tyre waste effects on the mixtures' collapsibility

To understand the collapse behaviour of quaternary soil mixed with rubber tyre waste, the specimens prepared in this study were tested using the double oedometer procedure. The volume changes were recorded for each effective normal stress and plotted as illustrated in Fig. 12a. Within the range of applied vertical stresses, all curves exhibit a clear upward concavity. In fact, for particulate systems, the concave stress-strain form is very characteristic; Lambe and Whitman [43] called such a form "locking." The impact of replacing the QS grains with the soft compressible TW and the inundation on resultant mixtures is clear in Fig. 12a. The dense pure QS reveals a high resistance in dry and soaked states as a result of its rigid grain nature. As the applied stress increases, collapse first occurs in the loose arrays and then in denser arrays in the soil. Thus, a further tight packing is the result of such movement; hence, the grains get stiffer and stiffer. However, this behaviour changes slightly with the inclusion of TW. The curves exhibit greater nonlinearity due to the inclusion of soft grains. With more inclusion, the stated state becomes more pronounced. For pure TW, due to its elastic deformability, even at lower applied stress, a large strain is produced.

On the other hand, the collapse potential (CP, %) at different effective stresses was also calculated, as shown in Fig. 12b. Limited collapse potential occurs in QS, its mixtures with lower TW, and in pure TW. While "moderate" to "moderately severe" collapse occurs for higher TW mixtures. The limited collapse observed in wetted QS is attributed to its rigid grain skeleton, low void ratio, and high stiffness. Inclusion TW allows grain rearrangement and causes a slight collapse. With further inclusion of soft grains, more replacement of the solid skeleton results in producing hybrid packing mixtures. The skeleton of such mixtures is weaker, allowing for more grain rearrangements, and as a result, a greater collapse (this is particularly pronounced for mixture QSTW45). On the other hand, the pure TR samples do not appear to undergo structural collapse due to the nature of the rubber, i.e., its hydrophobicity and resistance to water ingress.

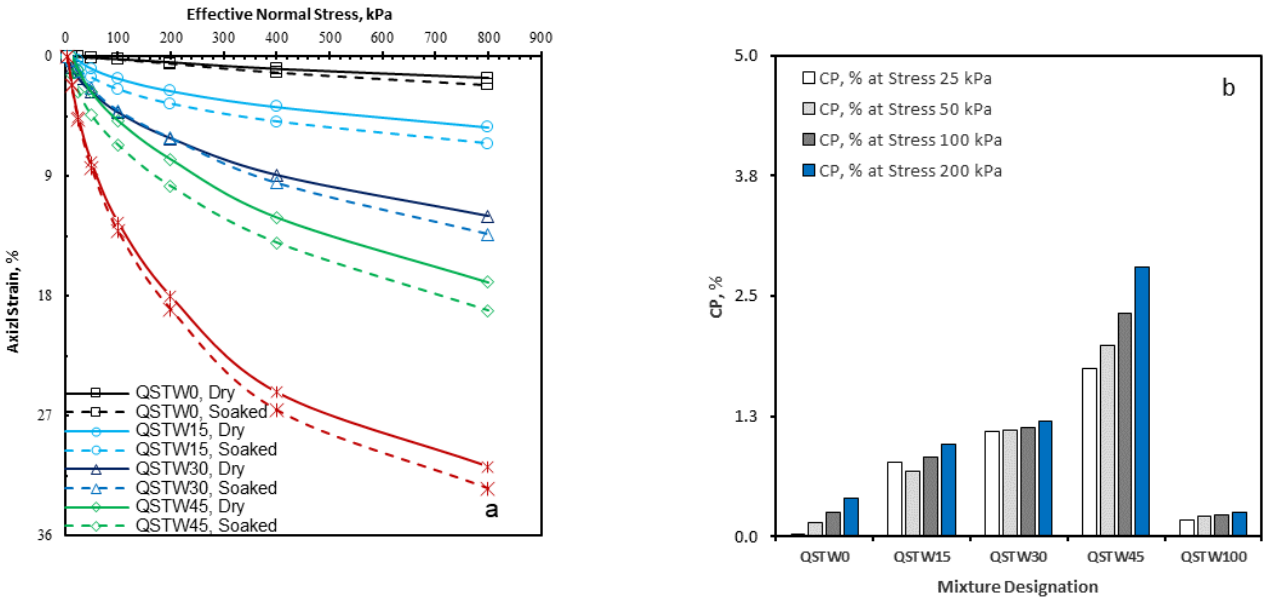

Fig. 12. Collapsibility of QSTW mixtures, a) axial strain versus. effective normal stress, b) collapse potential

3.4. Cyclic loading response of mixtures

In light of the energy-dissipating properties of rubber [64,65], the QSTW mixtures were investigated under confined compression conditions, in both dry and soaked states, and under cycles of loading – unloading – reloading, as illustrated in Fig. 13. As presented, there is a part of the strain recovered from that which occurred during the loading stage. The irreversible strain originates from particle fracturing or sliding. As soil is loaded, its particles store elastic energy. When these particles are unloaded, the energy causes them to rebound. Figure 13 also presents the reloading behaviour of mixtures that have been subjected to a cycle of loading and unloading. Two distinct responses were observed: one for mixtures loaded at a stress below the first maximum stress during initial loading, and another for mixtures loaded above this stress level. In the first one, the mixtures are stiffer after reloading than after the first loading. Since the particles of the mixture have already started sliding during the first loading. While in the second state, similar stress-strain curves to those that have not been subjected to unloading.

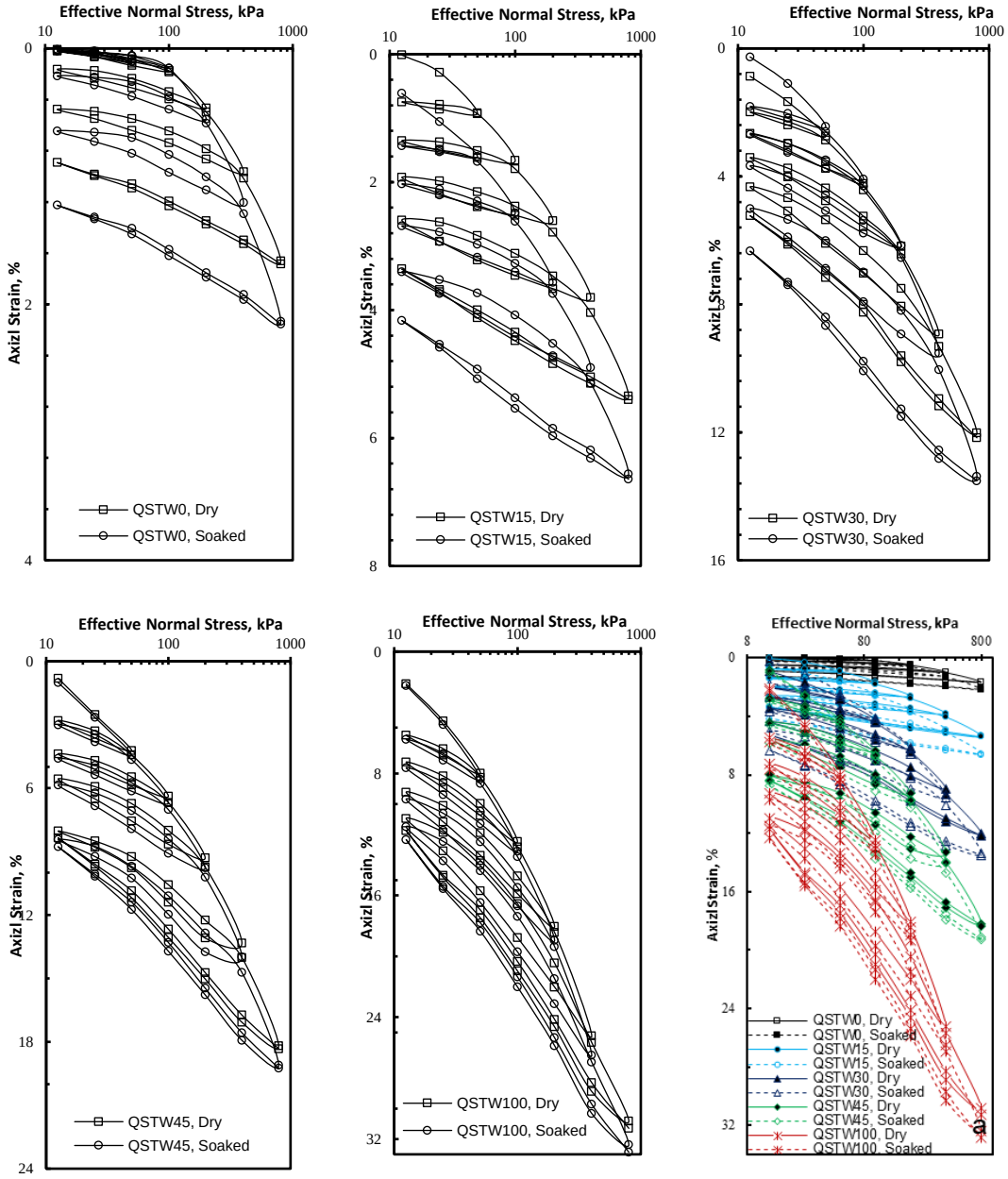

Fig. 13. Cycles of loading – unloading – reloading for QSTW mixtures

The loading–unloading–reloading cycles shown in Fig. 13 were used to examine the permanent and rebound strains of the pure QS, QSTW mixtures, and pure TW. These strains were calculated and are presented in Fig. 14. For pure QS, the rebound strain of the rigid sand grains is much greater compared to the permanent strain. It is about 57-89% of the total strain (the sum of permanent and rebound) for each cycle. This percentage, however, is influenced by the maximum load per cycle. For QSTW mixtures, the strain behaviour depends on the quantity of TW and the maximum loading stress. In the mixture of a lower TW, it was noted that the recoverable strain is lower than the permanent strain when the maximum loading stress is less than 200 kPa, and vice versa. As TW content increases, the loop with a maximum loading stress below 100kPa has a lower irrecoverable strain. This is also noted in pure rubber. The permanent strain values decrease with increasing cycles of loading-unloading-reloading.

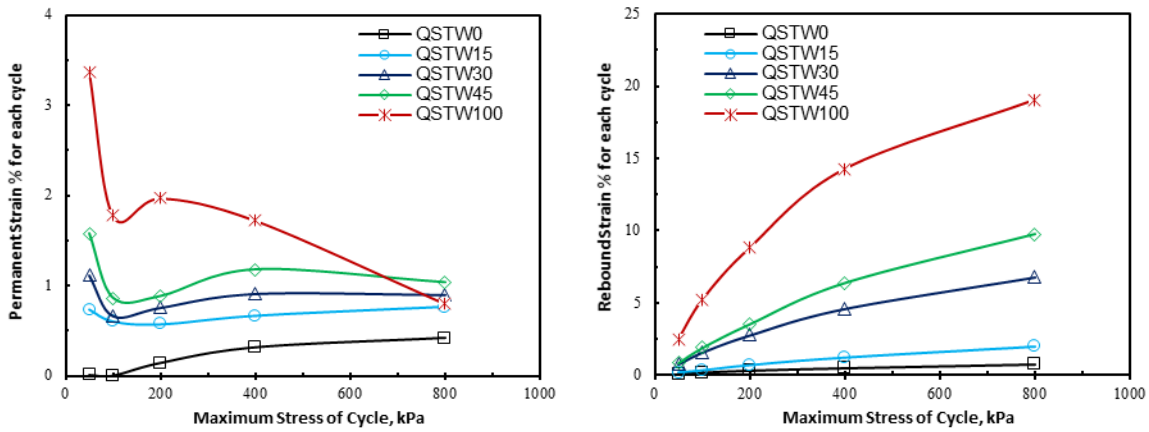

Fig. 14. The permanent stain and the rebound strain of QSTW mixtures

From a geotechnical perspective, the loading-unloading loops can provide insight into the energy dissipation and damping of the Quaternary soil-rubber tyre waste mixtures under the presented conditions. With respect to the dissipated energy, Fonseca et al. [38] mentioned that the energy can be obtained by measuring the area enclosed between the loading and the reloading curves for each loop of the oedometer loading-unloading cycles, as illustrated in Fig. 13. It is worth mentioning that the amount of energy dissipation calculated from the oedometer test is useful to provide comments on the nature of energy. However, to provide a precise measurement of energy dissipation, each test sample and the curves in a specific loading-unloading loop in Fig. 13 are subjected to nonlinear regression. The fitting using a polynomial function, cubic (Eq. 4), was applied to capture a smooth transition and the curvature of the progressive loading and unloading stages. This function is well-suited to capture the nonlinearity of the loading-unloading curves, and it remains analytically integrable. The loading branch is fitted separately from the unloading curve, utilising least-squares regression. The correlation parameters for the applied function are determined using NCSS 2025 [67] (advanced statistical software). The values of the constants (m_1, m_2, m_3, and m_4) and the statistical coefficients for Eq. 4 were determined. Excellent values of the determination coefficient (R^2) are obtained (greater than 96%), which indicate that the selected model is successfully approximating the non-linearity of curves for loops from the cyclic oedometer tests on QSTW mixtures.

$$\varepsilon_v = m_1\sigma_v^3 + m_2\,\sigma_v^2 + m_3\sigma_v + m_4 \qquad (4)$$

The obtained integrable polynomial functions enable the determination of the area enclosed in each loop. According to the scholars [68,69], the analytical integration of the function fitted to the stress-strain branches is the energy dissipated (D_E). Thus, the expression in Eq. 5 is used to determine the area of each loop in Fig. 13.

$$D_E = \int \varepsilon_v(\sigma)d\sigma = \int \varepsilon_{unloading}\,d\sigma - \int \varepsilon_{loading}\,d\sigma \qquad (5)$$

By substituting the constants from Eq. 4 for the loading and unloading curves and integrating the resulting equations in Eq. 5, the energy dissipated (per unit volume) for each loop (between the stresses' respective limits). Actually, the area below the loading branch is the absorbed energy; meanwhile, below the unloading branch is the "released energy." Both energies can be estimated using Eq. 5. Thus, the area for each loop was estimated to represent the D_E. Keeping in mind, the amounts of calculated energy are applicable to provide comments regarding the nature of energy.

To illustrate the effect of TW and facilitate comparison, the values of D_E for each mixture were normalised with respect to the D_E of TW from each loop, as in Table 2. The characteristics of the pure materials have a major role in the dissipated energy of their mixtures. As noted, the high recovery tendency of TW under compression, its low stiffness, and its high deformability compared to QS contribute to the distinct damping behaviour of the QS–TW mixtures.

Table 2. The variation of the normalized energy dissipation with different rubber fractions

Mixture	State	Loop of loading and unloading (stress in kPa)				
		12.5 to 50	12.5 to 100	12.5 to 200	12.5 to 400	12.5 to 800
QSTW0	Dry	0.01	0.02	0.07	0.07	0.12
	Soaked	0.01	0.01	0.12	0.10	0.19
QSTW15	Dry	0.16	0.22	0.23	0.14	0.26
	Soaked	0.22	0.27	0.25	0.15	0.33
QSTW30	Dry	0.34	0.45	0.68	0.35	0.37
	Soaked	0.54	0.49	0.72	0.42	0.40
QSTW45	Dry	0.43	0.50	0.58	0.53	0.83
	Soaked	0.63	0.71	0.66	0.54	0.83
QSTW100	Dry	1.00	1.00	1.00	1.00	1.00
	Soaked	1.00	1.00	1.00	1.00	1.00

Dissipated energy (D_E) reflects the internal friction and permanent deformation of geomaterials under cyclic loading. The D_E represents the work lost by the material during each loading cycle. The energy is associated with the geomaterials' capacity to dampen the vibrations caused by dynamic loads. In combinations of rubber materials and granular geomaterials, damping and energy dissipation are directly proportional. The interfacial friction, particle rearrangement, and viscoelastic hysteresis of the TW grains are the mechanisms governing the damping and energy dissipation of such mixes. The cyclic odometer's loop-loading and unloading curves allow straightforward evaluation of the D_E. Mixtures with a larger loop area should dissipate more energy. From Fig. 13 and Table 2, it is evident that the inclusion of TW soft grains in the mixture of QS enhances the energy dissipated. The generated mixes gain increased viscoelastic resistance and deformability as a result of this inclusion. However, this depends on the magnitude of the applied stresses. At low to moderate stress levels (less than 400 kPa), the TW particles and the QS skeleton both experience simultaneous compression and rearrangement. Higher stresses cause TW grains to compress strongly, thereby enlarging the loading – unloading loop area and increasing energy dissipation. Under very high strains, the mixtures become denser, with both QS and TW grains compacting substantially, resulting in additional energy release.

This work examines the impact of saturation on the energy dispersion of QSTW mixtures. The loading-unloading loops were produced for both dry and soaked mixtures, as shown in Fig. 15. Overall, saturation has a negligible effect on energy dissipation. Soaking causes a slight reduction in the loading-unloading loop area at stress levels between 50 and 100 kPa. At a stress level of 100 kPa, however, less severe changes are observed. Additionally, mixtures loaded to 200 and 400 kPa showed slight variations in DE compared to the unsoaked state. At 800 kPa, however, the viscoelastic behaviour of TW primarily governs the dissipated energy [35,66,70–71].

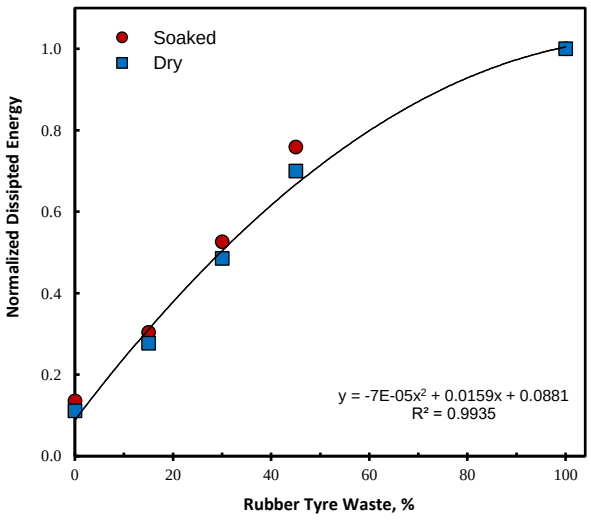

Fig. 15. Normalised energy dissipation with different rubber fractions

4. Conclusions

The compressibility, stiffness, and energy dissipation of Quaternary soil-rubber tyre waste Mixtures Under lateral restraint conditions have been analysed and deduced. Accordingly, conclusions from the results are drawn as shown

1. The mixes exhibit high compressibility and increased deformation with higher TW content, reaching a minimum void ratio of approximately 0.2. When the applied stresses exceed 400 kPa, and the mixtures contain more than 30% TW, the compressibility curves appear to be more nonlinear. Moreover, at the end of the unloading stages, higher rebound deformation values are observed. Cc and Cr almost increase linearly with increasing TW content, whereas the pattern is nonlinear with decreasing rubber content.
2. Because rubber grains are less stiff and elastically deformable, the normal stress-axial strain curves become increasingly nonlinear with higher TW content. Sand-like behaviour predominates, and the stiffness parameter decreases with decreasing TW content because rubber particle contacts are less prevalent. However, the stiffness of the QSTW mixtures is insignificantly affected by the soaking.
3. Due to its stiff structure, high stiffness, rigid skeleton, and low void ratio, wetted QS exhibits minimal collapse. As the TW inclusion grows, the CP rises as well, permitting grain rearrangement and resulting in a slight collapse (less than 2%). Hybrid packing combinations are created when soft TW materials are added in greater quantities, replacing the solid skeleton. The weaker skeleton in these mixtures permits greater grain rearrangement, leading to increased collapse. However, because of their hydrophobic nature and resistance to water intrusion, the pure TW samples do not appear to undergo structural collapse.
4. The QSTW mixtures absorb and release more energy as a result of the TW incorporation. Within the mixtures, the TW functioned as a miniature damper. The loading and unloading loops in the cyclic oedometer tests make this evident. Additionally, when the TW fraction increases, the unloading branch becomes more curved, indicating a more gradual response, while the loading curves flatten. In contrast, pure QS exhibits a narrow loop with minimal energy dissipation, as the loading and unloading branches are closer together. This explains the viscoelastic character of TW particles and the rise in the interface slip between QS and TW.

Ultimately, the QSTW mixtures' increased damping capacity proves their further use. They can be used in a variety of infrastructure applications to reduce seismic strain on retaining structures and to dampen foundation vibrations. Mitigating seismic loading impacts through isolation techniques for retaining structures and foundations is an emerging trend. The potential of QSTW mixtures as a sustainable solution warrants investigation in engineering practice.

Finally, it should be noted that the present study focuses on a geotechnical perspective and is applicable to small samples of poorly graded fine-quaternary sand mixed with up to 45% rubber from scrap tyres. Beyond this limit, further investigation is worthy to conduct. Moreover, to facilitate the application of sand-rubber mixtures in real applications that mitigate dynamic/seismic excitations, it is recommended to further investigate the limitations and requirements for estimating the thickness of the QSTW layer to achieve a proper mitigation effect.

Funding

The authors declared that no grants were involved in supporting this work.

References

[1] Culshaw M.G., Cripps J.C., Bell F.G., Moon C.F., Engineering Geology of Quaternary Soils: I. Processes and Properties, *Engineering Geology Special Publications* 7 (1991) 3- 38. https://doi.org/10.1144/GSL.ENG.1991.007.01.01

[2] Al-Taie A.J., Statistical Method for estimating Selected Geotechnical Properties of Quaternary Sediment, *Konya Journal of Engineering Sciences (KONJES)* 11(4) (2023) 928-941. https://doi.org/10.36306/konjes.891806

[3] Al-Taie A.J., Al-Jeznawi D., Faraj N., Engineering Characterization of Quaternary Sandy Soil in the Mesopotamia Plain, I*nternational Review of Civil Engineering (IRECE)* 12(1) (2021) 40-48. https://doi.org/10.15866/irece.v12i1.18770

[4] Al-Taie A., Ahmed M., Selection Considerations and Classification Bases of Earth Retaining Systems, *Jurnal Kejuruteraan (Journal of Engineering)* 37(2) (2025) 679-694. https://doi.org/10.17576/jkukm-2025-37(2)-11

[5] Anastasiadis A., Senetakis K., Pitilakis K., Gargala C., Karakasi I., Dynamic Behavior of Sand/Rubber Mixtures. Part I: Effect of Rubber Content and Duration of Confinement on Small-Strain Shear Modulus and Damping Ratio, *Journal of ASTM International* 9(2) (2012) 1-19. https://doi.org/10.1520/JAI103680

[6] Fiamingo A., Chiaro G., Murali A., Massimino M., Geotechnical Characterization of Soil-Rubber Mixtures With Well-Graded Gravel, *Geosynthetics International* 32(6) (2025) 818–834. https://doi.org/10.1680/jgein.24.00177

[7] Oleiwi S. and Albayati A., Incorporating Recycled Crumb Rubber into Asphalt: A Comprehensive Review, *Journal of Engineering* 30(10) (2024) 184–202. https://doi.org/10.31026/j.eng.2024.10.11

[8] Al-Fayyadh Z., Al-Mosawe H., The Effect of Rubber Crumbs on Marshall Properties for Warm Mix Asphalt, *Journal of Engineering* 29(6) (2023) 46–59. https://doi.org/10.31026/j.eng.2023.06.04

[9] Hasan T., Ali A., Flexural Behavior of Fiber Reinforced Self-Compacting Rubberized Concrete Beams, *Journal of Engineering* 26(2) (2020) 111–128. https://doi.org/10.31026/j.eng.2020.02.09

[10] Ahmed I., Lovell C.W., Rubber Soils as Lightweight Geomaterials. In Lightweight Artificial and Waste Materials for Embankments Over Soft Soils, *Transportation Research Record* 1422 (1993) 61–70. https://onlinepubs.trb.org/Onlinepubs/trr/1993/1422/1422-010.pdf

[11] Pitilakis K., Karapetrou S., Tsagdi K., Numerical Investigation Of The Seismic Response Of RC Buildings On Soil Replaced With Rubber–Sand Mixtures, *Soil Dynamics and Earthquake Engineering* 79(A) (2015) 237-252. https://doi.org/10.1016/j.soildyn.2015.09.018

[12] Edincliler A., Baykal G., Dengili K., Determination of Static and Dynamic Behavior of Recycled Materials for Highways, *Resour Conser Recycl* 42(3) (2004) 223–237. https://doi.org/10.1016/j.resconrec.2004.04.003

[13] ElEmbaby A., Nassar A., Elawsya M., Impact of Silica Nanoparticles Incorporation on the Properties of Resin Infiltration: An in Vitro Study, *BMC Oral Health* 24 (2024) 1484. https://doi.org/10.1186/s12903-024-05107-7

[14] Khan M., Ahmad J., Khan H., Umer M., High Strength Rubberized Porous Concrete for Sustainable Pavements: Engineering Properties and Life Cycle Assessment, *Journal of Cleaner Production* 451 (2024) 142012. https://doi.org/10.1016/j.jclepro.2024.142012

[15] Feng Z., Sutter K., Dynamic Properties of Granulated Rubber/Sand Mixtures, *Geotechnical Testing Journal* 23(3) (2000) 338–344. https://doi.org/10.1520/GTJ11055J

[16] Abdelaleem A., Moawad M., El-Emam H., Salim H., Sallam H., Long Term Behavior of Rubberized Concrete Under Static and Dynamic Loads, *Case Studies in Construction Materials* 20, (2024) e03087. https://doi.org/10.1016/j.cscm.2024.e03087

[17] Olofinnade O., Adeyinka O., The Utilization of Pulverized Waste Tire Rubber in a Soil–Cement Composite for Sustainable Compressed Earth Brick Production, *Discover Civil Engineering* 1(69) (2024). https://doi.org/10.1007/s44290-024-00075-x

[18] Ghaleh M., Asadi P., Eftekhar M., Life cycle Assessment Based Method for the Environmental and Mechanical Evaluation of Waste Tire Rubber Concretes, *Scientific Reports* 15 (2025) 10687. https://doi.org/10.1038/s41598-025-95850-w

[19] Edincliler A., Baykal G., Saygili A., Influence of Different Processing Techniques on the Mechanical Properties of Used Tires in Embankment Construction, *Waste Management* 30(6) (2010) 1073–1080. https://doi.org/10.1016/j.wasman.2009.09.031

[20] Heimdahl C., Druscher A., Elastic Anisotropy of Tire Shreds, *Journal of Geotechnical and Geoenvironmental Engineering* 125(5) (1999) 383–389. https://doi.org/10.1061/(ASCE)1090-0241(1999)

[21] Akhtar A., Tsang H., A Comparative Life Cycle Assessment of Recycled Tire Rubber Applications in Sustainable Earthquake-Resistant Construction, *Resources, Conservation and Recycling* 211 (2024) 107860. https://doi.org/10.1016/j.resconrec.2024.107860

[22] Lin G., Liu W., Yang F., Experimental Investigation of the Mechanical Behaviour of Sand-Rubber-Gravel Mixtures, *Bulletin of Engineering Geology and the Environment* 84 (2025) 74. https://doi.org/10.1007/s10064-025-04109-1

[23] Oh J., Choo H., Thermal Conductivity of Sand–Tire Rubber Mixtures as a Function of Tire Chip Fraction, Size Ratio, Void Ratio and Applied Vertical Stress, *Acta Geotechnica* 20 (2025) 2927–2942. https://doi.org/10.1007/s11440-025-02597-9

[24] Wang P., Gan J., Huang S., Micro-Mechanical Analysis of Sand-Rubber Mixtures with discrete Element Method, *Acta Geotechnica* 20 (2025) 4289–4309. https://doi.org/10.1007/s11440-025-02670-3

[25] ASTM International, ASTM D6270-20., *Standard Practice for Use of Scrap Tires in Civil Engineering Applications*, Annual Book of ASTM Standard, Vol.n11.04, 2020. https://doi.org/10.1520/D6270-20

[26] Tsang H., Analytical Design Models for Geotechnical Seismic Isolation Systems, *Bulletin of Earthquake Engineering* 21 (2022) 3881–3904. https://api.semanticscholar.org/CorpusID:251043071

[27] Forcellini D., Assessment on Geotechnical Seismic Isolation (GSI) on Bridge Configurations, *Innovative Infrastructure Solutions* 2 (2017) 760. https://doi.org/10.1007/s41062-017-0057-8

[28] Tsiavos A., Kolyfetis D., Panzarasa G., Burgert I., Stojadinovic B., Shaking Table Investigation of a Low-Cost and Sustainable Timber-Based Energy Dissipation System with Recentering Ability, *Bulletin of Earthquake Engineering* 21(8) (2022) 3949–3968. https://doi.org/10.1007/s10518-022-01464-2

[29] Pitilakis D., Anastasiadis A., Vratsikidis A., Kapouniaris A., Massimino M.R., Abate G., Corsico S., Large-scale Field Testing of Geotechnical Seismic Isolation of Structures Using Gravelrubber Mix- Tures. Earthquake Engineering & Structural Dynamics 50(10) (2021) 2712–2731. https://doi.org/10.1002/eqe.3468

[30] Maleska T., Bęben D., Vaslestad, J., Long-Term Monitoring of Earth Pressure in a Soil-Steel Composite Railway Tunnel, In J.S. Jensen, D.M. Frangopol, & J.W. Schmidt (Eds.), Bridge maintenance, safety, management, digitalization and sustainability, (2024) 1296–1303. CRC Press/Balkema. https://doi.org/10.1201/9781003483755-150

[31] Bernal A., Lovell C. W., Salgado R., *Laboratory study on the use of tire shreds and rubber-sand in backfills and reinforced soil applications*, Publication FHWA/IN/JHRP-96/12. Joint Highway Research Project, Indiana Department of Transportation and Purdue University, West Lafayette, Indiana, 1996. https://doi.org/10.5703/1288284313259

[32] Edil T.B., Bosscher P.T., Eldin N.N., *Development of Engineering Criteria for Shredded or Whole Tires in Highway Applications*, Department of Civil and Environmental Engineering, University

of Wisconsin-Madison, Wisconsin, 1990, 19. https://scholar.google.com/scholar_lookup?title=Development+of+engineering+criteria+for+shredded+or+whole+tires+in+highway+applications&author=T.+B.+Edil&author=P.+J.+Bosscher&author=N.+N.+Eldin&publication_year=1990

[33] Humphrey D.N., Manion W.P., Properties of Tire Chips for Lightweight Fill, *Grouting, Soil Improvement and Geosynthetics* ASCE, American Society of Civil Engineers, New York, Geotechnical Special Publication 30(2) (1992) 1344-1355.

[34] Humphrey D.N., Sandford T.C., Cribbs M.M., Gharegrat H., Manion W. P., Shear Strength and Compressibility of Tire Chips for Use as Retaining Wall Backfill, *Transportation Research Board*, Transportation Research Record 1422 (1993) 29-35. https://onlinepubs.trb.org/Onlinepubs/trr/1993/1422/1422-006.pdf

[35] Fonseca J., Riaz A., Bernal-Sanchez J., Barreto D., McDougall J., Miranda-Manzanares M., Marinelli A., Dimitriadi V., Particle–Scale Interactions and Energy Dissipation Mechanisms in Sand–Rubber Mixtures, *Geotechnique Letters* 9(4) (2019) 263–268. https://doi.org/10.1680/jgele.18.00221

[36] Wu Q., Ma W., Liu O., Zhao K., Chen G., Dynamic Shear Modulus and Damping Ratio of Rubber-Sand Mixtures with a Wide Range of Rubber Content, *Materials Today Communications* 27 (2021) 102341. https://doi.org/10.1016/j.mtcomm.2021.102341

[37] Anastasiadis A., Senetakis K., Pitilakis, K., Small-Strain Shear Modulus and Damping Ratio of Sand-Rubber and Gravel-Rubber Mixtures, *Geotechnical and Geological Engineering* 30 (2012) 363–382. https://doi.org/10.1007/s10706-011-9473-2

[38] Ozkan S., Ibraim E., Diambra A., Sand-rubber Mixtures Under One-Dimensional Cyclic Loading, in: Geosynthetics: Leading the Way to a Resilient Planet, 2023a, 344-350. https://doi.org/10.1201/9781003386889-27

[39] Tao H., Zheng W., Zhou X., Zhou L., Li C., Yu Y., Jiang P., Study on Dynamic Modulus and Damping Characteristics of Modified Expanded Polystyrene Lightweight Soil under Cyclic Load, *Polymers* 15(8) (2023) 1865. https://doi.org/10.3390/polym15081865

[40] Li X., Yang Y., Bie J., Wang J., Liu E., Undrained Cyclic Behavior of Rubber-Sand Mixture Under Multi-Directional Loads, *Case Studies in Construction Materials* 20 (2024) e03258. https://doi.org/10.1016/j.cscm.2024.e03258

[41] Polito C., Zhang Z., Moldenhauer H., Dissipation of Energy and Generation of Pore Pressure in Load-Controlled and Displacement-Controlled Cyclic Tests, *Geotechnics* 4(4) (2024) 1026-1047. https://doi.org/10.3390/geotechnics4040052

[42] Polito C., Martin J., Dissipated Energy and Pore Pressure Generation Patterns in Sands and Non-Plastic Silts Subjected to Cyclic Loadings, Geotechnics 4(1) (2024) 264-284. https://doi.org/10.3390/geotechnics4010014

[43] Lambe W., Whitman R., *Soil Mechanics*, John Wiley & Sons, 1979. https://www.scribd.com/document/356518709/63874574-Soil-Mechanics-by-Lambe-and-Whitman-pdf

[44] ASTM International, ASTM D2487-17E01, *Standard Practice for Classification of Soils for Engineering Purposes (Unified Soil Classification System)*, Annual Book of ASTM Standard 4.08, 2025. https://doi.org/0.1520/D2487-17E01

[45] ASTM International, ASTM D854-23, *Standard Test Methods for Specific Gravity of Soil Solids by the Water Displacement Method*, Annual Book of ASTM Standard 4.08, 2023. https://doi.org/10.1520/D0854-23

[46] ASTM International, ASTM D422., *Standard Test Method for Particle-Size Analysis*, Annual Book of ASTM Standard 4.08, 2017. https://doi.org/10.1520/D0422-63R98

[47] ASTM International, ASTM D4253., *Standard Test Methods for Maximum Index Density and Unit Weight of Soils Using a Vibratory Table*, Annual Book of ASTM Standard 4.08, 2021. https://doi.org/10.1520/D6270-20

[48] ASTM International, ASTM D4254., *Standard Test Methods for Minimum Index Density and Unit Weight of Soils and Calculation of Relative Density*, Annual Book of ASTM Standard 4.08, 2017. https://doi.org/ 10.1520/D4253-00

[49] ASTM International, ASTM D2435., *Standard Test Methods for One-Dimensional Consolidation Properties of Soils Using Incremental Loading*, Annual Book of ASTM Standard 4.08, 2011. https://doi.org/ 10.1520/D2435-04

[50] ASTM International, ASTM D2488-17E01, *Standard Practice for Description and Identification of Soils (Visual-Manual Procedures)*, Annual Book of ASTM Standard 4.08, 2025. https://doi.org/10.1520/D2488-17E01.

[51] Jennings J.E., Knight K., The Additional Settlement of Foundation Due to Collapse of Sandy Subsoils on Wetting, in Proc. 4th ICSMFE 1 (1957) 316-319. https://www.issmge.org/uploads/publications/1/41/1957_01_0066.pdf

[52] Edil T.B., Bosscher P.T., Engineering Properties of Tire Chips and Soil Mixtures, *Geotechnical Testing Journal* 17(4) (1994) 453-464. https://doi.org/10.1520/GTJ10306J

[53] Ozkan S., Ibraim E., Diambra A., Sand Rubber Mixtures: 1D Compressibility Response. in Y. Yukselen-Aksoy et al. (eds.), Sustainable Earth and Beyond, *Lecture Notes in Civil Engineering* 370 (2023b), https://doi.org/10.1007/978-981-99-4041-7_16

[54] Lee J., Dodds J., Santamarina J., Behavior of Rigid-Soft Particle Mixtures, *Journal of Materials in Civil Engineering* 19(2) (2007) 179–184. https://doi.org/10.1061/(ASCE)0899-1561(2007)19:2(179)

[55] Kim H., Santamarina J., Sand–rubber Mixtures (Large Rubber Chips), *Canadian Geotechnical Journal* 45(10) (2008) 1457–1466. https://doi.org/10.1139/T08-070

[56] Rouhanifar S., *Mechanics of soft-rigid soilmixtures*, Department of Civil Engineering. University of Bristol, Bristol, 2015. https://www.researchgate.net/publication/305710419_Mechanics_of_soft-rigid_soil_mixtures

[57] Sheikh M., Mashiri M., Vinod J., Tsang H., Shear and Compressibility Behavior of Sand-Tire Crumb Mixtures, *Journal of Materials in Civil Engineering* 25(10) (2013) 1366–1374. https://doi.org/10.1061/(ASCE)MT.1943-5533.0000696

[58] Muir-Wood D., *Soil mechanics: a one-dimensional introduction*, Cambridge University Press, New York, 2009. https://doi.org/10.1017/CBO9780511815553

[59] Lee C., Shin H., Lee J., Behavior of Sand-Rubber Particle Mixtures: Experimental Observation and Numerical Simulations, *International Journal for Numerical and Analytical Methods in Geomechanics* 38(16) (2014) 1651–1663. https://doi.org/10.1002/nag.2264

[60] Liu L., Cai G., Liu S., Compression Properties and Micro-Mechanisms of Rubber-Sand Particle Mixtures Considering Grain Breakage, *Construction Building Materials* 187(1) (2018) 1061–1072. https://doi.org/10.1016/j.conbuildmat.2018.08.051

[61] Holtz R.D., Kovacs W.D., Sheahan T.C., *An introduction to geotechnical engineering*, Third Edition, Pearson Education, Inc, Hoboken, 2023. https://www.vitalsource.com/en-ca/products/introduction-to-geotechnical-engineering-an-robert-d-holtz-william-d-v9780135619421?srsltid=AfmBOoq-Mj95UG2oCWxr5_CPQhLs5TQYauFew6Tm1VSEmOnwRxBOt_UB

[62] Madhusudhan B., Boominathan A., Banerjee S., Engineering Properties of Sand–Rubber Tire Shred Mixtures, *International Journal of Geotechnical Engineering* 15(5) (2019) 1061–1077. https://doi.org/10.1080/19386362.2019.1617479

[63] Lee C., Truong Q., Lee W., Lee J., Characteristics of Rubber-Sand Particle Mixtures According to Size Ratio, *ournal of Materials in Civil Engineering* 22(4) (2010) 323–331. https://doi.org/10.1061/(ASCE)MT.1943-5533.0000027

[64] Liu X., Chaoyang T., Hengxin L., Laboratory Investigation of the Mechanical Properties of a Rubber–Calcareous Sand Mixture: The Effect of Rubber Content, *Applied Sciences* 10(18) (2020) 6583. https://doi.org/10.3390/app10186583

[65] Han L., Wei H., Wang F., Study on the Vibration Isolation Performance of Composite Subgrade Structure in Seasonal Frozen Regions, *Applied Sciences* 10(10) (2020) 3597. https://doi.org/10.3390/app10103597

[66] Li J., Cui J., Shan Y., Li Y., Ju B., Dynamic Shear Modulus and Damping Ratio of Sand–Rubber Mixtures under Large Strain Range, *Materials* 13(18) (2020) 4017. https://doi.org/10.3390/ma13184017

[67] *NCSS Statistical Software*, NCSS, LLC. Kaysville, Utah, USA, 2025. https://www.ncss.com/

[68] Jiang P., Shaowie L., Wang Y., Li N., Wang W., Investigation on Direct Shear and Energy Dissipation Characteristics of Iron Tailings Powder Reinforced by Polypropylene Fiber, *Applied Sciences* 9(23) (2019) 5098. https://doi.org/10.3390/app9235098

[69] Al-Taie A.J., Shear Strength Augmentation and Energy Dissipation for Uniformly Graded Soil, in *International Middle Eastern Simulation and Modelling Conference*, *MESM 2024*, 2025 77–82. https://www.scopus.com/pages/publications/105003232681?origin=resultslist

[70] Dai B., Chen Y., Chang D., Yang J. , Liu J., Experimental Study on the Critical-State and Energy Dissipation Behaviors of Rubber-Sand Mixtures, *International Journal of Geomechanics* 24(3) (2023). https://doi.org/10.1061/IJGNAI.GMENG-8818

[71] Dai B., Liu Q., Mao X., Li P., Liang Z., A Reinterpretation of the Mechanical Behavior of Rubber-Sand Mixtures in Direct Shear Testing, *Construction and Building Materials* 363 (2024) 129771. https://doi.org/10.1016/j.conbuildmat.2022.129771